

# Supporting information for: Single-layer plasmonic metasurface half-wave plates with wavelength-independent polarization conversion angle

Zhaocheng Liu,<sup>†</sup> Zhancheng Li,<sup>†</sup> Zhe Liu,<sup>‡</sup> Hua Cheng,<sup>†</sup> Wenwei Liu,<sup>†</sup> Chengchun  
Tang,<sup>‡</sup> Changzhi Gu,<sup>‡</sup> Junjie Li,<sup>‡</sup> Hou-Tong Chen,<sup>¶</sup> Shuqi Chen,<sup>\*,†</sup> and Jianguo  
Tian<sup>†</sup>

<sup>†</sup>*The Key Laboratory of Weak Light Nonlinear Photonics, Ministry of Education, School of Physics and TEDA Institute of Applied Physics, Nankai University, Tianjin 300071, China.*

<sup>‡</sup>*Beijing National Laboratory for Condensed Matter Physics, Institute of Physics, Chinese Academy of Sciences, P.O.Box 603, Beijing 100190, China.*

<sup>¶</sup>*Center for Integrated Nanotechnologies, Los Alamos National Laboratory, Los Alamos NM87545, USA*

E-mail: schen@nankai.edu.cn; URL: <http://chenlab.nankai.edu.cn>

We discuss the theoretical formulation on the plasmonic half-wave plates in section 1 with Equations S1-S10. The polarization conversion of sample E, the analysis of state-of-polarization of all samples, the bandwidth of the metasurface half-wave plates, the experimental manifestation of symmetrical property and a schematic configuration of the experimental setup are displayed in section 2 with figures S1-S5.

# 1 Supplementary equations: Theoretical Formulation on the plasmonic half-wave plates

Our metasurface can be analytically demonstrated as a half-wave plate using the Jones Matrix at any incident polarization. Suppose the anisotropic nanoantenna pair positioned at an angle  $\varphi_1$  and  $\varphi_2$  with respect to the  $x$  axis, exert operations  $P(\varphi_1)$  and  $P(\varphi_2)$  to the incident light, then their function (in the form of operator) can be written as:

$$P(\varphi_1) |L\rangle = \alpha |L\rangle + \beta |R\rangle e^{-i2\varphi_1} \quad (\text{S1})$$

$$P(\varphi_1) |R\rangle = \alpha |R\rangle + \beta |L\rangle e^{i2\varphi_1} \quad (\text{S2})$$

$$P(\varphi_2) |L\rangle = \alpha |L\rangle + \beta |R\rangle e^{-i2\varphi_2} \quad (\text{S3})$$

$$P(\varphi_2) |R\rangle = \alpha |R\rangle + \beta |L\rangle e^{i2\varphi_2} \quad (\text{S4})$$

where  $\alpha$  and  $\beta$  are the conversion efficiencies of the circularly-polarized light. We define a ‘‘constant angle’’  $\Delta$  expressed as  $\Delta = \varphi_1 + \varphi_2$ , and set  $\varphi_1 = \varphi$  for convenience. Then Equation S1 and S2 can be rewritten as:

$$P(\varphi_1) |L\rangle = \alpha |L\rangle + \beta |R\rangle e^{-i2\varphi} \quad (\text{S5})$$

$$P(\varphi_1) |R\rangle = \alpha |R\rangle + \beta |L\rangle e^{i2\varphi} \quad (\text{S6})$$

$$P(\varphi_2) |L\rangle = \alpha |L\rangle + \beta |R\rangle e^{i2\varphi - i2\Delta} \quad (\text{S7})$$

$$P(\varphi_2) |R\rangle = \alpha |R\rangle + \beta |L\rangle e^{-i2\varphi + i2\Delta} \quad (\text{S8})$$

Suppose an arbitrarily polarized light, denoted in Dirac notation as  $|E_{in}\rangle = \begin{bmatrix} A \\ Be^{i\delta} \end{bmatrix}$  (where  $A$  and  $B$  are amplitudes in the  $x$  and  $y$  directions,  $\delta$  is the phase difference between them), is cast onto the two nanoantennas. The transmitted light thus can be denoted as

$|E_{out}\rangle = [P(\varphi_1) + P(\varphi_2)] |E_{in}\rangle$ . Substituting  $P(\varphi_1)$  and  $P(\varphi_2)$  into  $|E_{out}\rangle$ , we can derive the expression after simplification as:

$$\begin{aligned}
|E_{out}\rangle &= \frac{\beta}{2} [(A + iBe^{i\delta}) |R\rangle + (A - iBe^{i\delta}) |L\rangle e^{i2\Delta}] e^{-i2\varphi} \\
&+ \frac{\beta}{2} [(A - iBe^{i\delta}) |L\rangle + (A + iBe^{i\delta}) |R\rangle e^{-i2\Delta}] e^{i2\varphi} \\
&+ 2\alpha |E_{in}\rangle
\end{aligned} \tag{S9}$$

To show the polarization states in Equation S9, we can substitute the expression of LCP state  $|L\rangle = \begin{bmatrix} 1 \\ -i \end{bmatrix}$  and RCP state  $|R\rangle = \begin{bmatrix} 1 \\ i \end{bmatrix}$  into Equation S9. Then  $|E_{out}\rangle$  changes to:

$$\begin{aligned}
|E_{out}\rangle &= \alpha \begin{bmatrix} 1 & 0 \\ 0 & 1 \end{bmatrix} \begin{bmatrix} A \\ Be^{i\delta} \end{bmatrix} + \\
&\beta \begin{bmatrix} \cos \Delta & \sin \Delta \\ \sin \Delta & -\cos \Delta \end{bmatrix} \begin{bmatrix} A \\ Be^{i\delta} \end{bmatrix} \cos(2\varphi - \Delta)
\end{aligned} \tag{S10}$$

This expression indicates that the original polarization state  $|E_{in}\rangle$  is linearly transformed to the  $|E_{out}\rangle$  by a device whose Jones matrix is  $H(\Delta) = \begin{bmatrix} \cos \Delta & \sin \Delta \\ \sin \Delta & -\cos \Delta \end{bmatrix}$ , which represents a half-wave plate with the optical axis oriented along  $\Delta/2$ , i.e., the bisection of the two nanoantennas,  $\frac{1}{2}(\varphi_1 + \varphi_2)$ .

## 2 Supplementary Figures

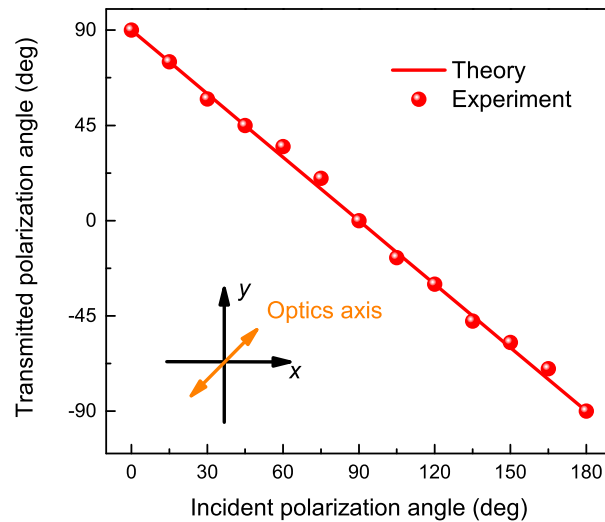


Figure S1: Polarization conversion of sample E. Besides the experimental demonstration of sample A, the results on Sample E in the circumstances of varying incident polarization direction are also presented here. The theoretical (line) and experimental (dots) transmitted polarization angles are shown as functions of incident polarization angle, Inset: The optical axis of Sample E.

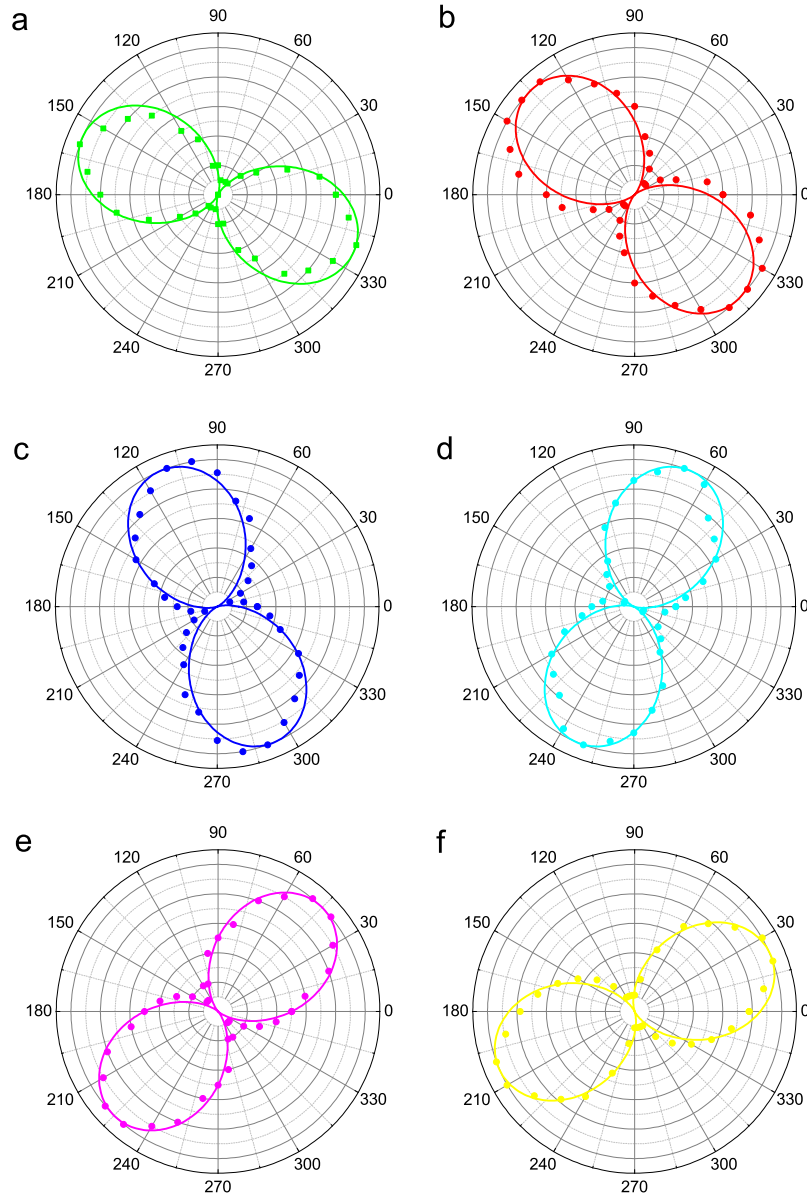


Figure S2: Analysis of state-of-polarization of all samples. (a)-(f) State-of-polarization analysis of the transmitted image light for sample B,C,D,F,G,H when the incident light is linearly polarized  $0^\circ$  at wavelength 980 nm. The dots are experimental results, and the solid lines are obtained from analytical calculations based on an ideal classical half-wave plate with the same optical axis as the corresponding metasurface half-wave plate. The good correspondence again proves the feasibility to regard our metasurfaces as high DOLP half-wave plates.

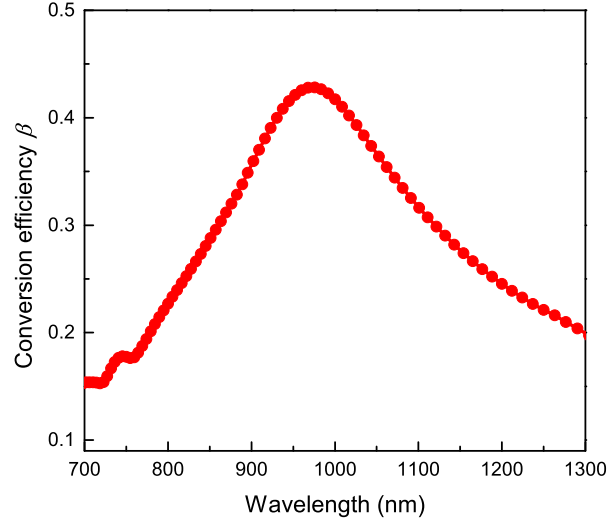


Figure S3: Bandwidth of the metasurface half-wave plates. The simulated value for  $\beta$  as a function of wavelength from 700 nm to 1300 nm. The only influence caused by  $\beta$  is the amplitude of the image light. The simulations were performed by detecting the RCP/LCP amplitude when the incident light is LCP/RCP. The resonant wavelength is 980 nm, where the maximum conversion efficiency is about 0.44. With the increasing or decreasing of the wavelength, the conversion efficiency shows a drop. The available band where amplitude decreases to half of the maximum is about from 820 nm to 1220 nm, guaranteeing a bandwidth of 400 nm. The interval distance between two antennas only affects the near-field coupling, and changes the resonance and bandwidth of whole device, so we neglected the effect of distance between two nanoantennas in the discussion.

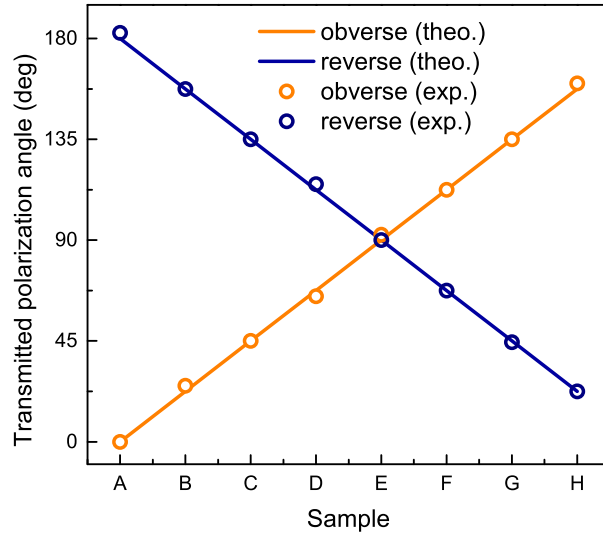


Figure S4: Experimental manifestation of symmetrical property. The polarization angle of the image light for all samples is measured when the incident light is cast on obverse (orange colored) and reverse (blue colored) sides of the samples. Lines and circles indicate the theory and experiment results, respectively, of the polarization angle of the image light when the incident polarization angle is set to zero. The results show that they have the same symmetry property as in classical half-wave plates. Different samples exhibit the variation of optical axis from  $0$  to  $\pi/2$ , thus the polarization angle of the transmitted image light varies from  $0$  to  $\pi$  at the intervals of  $\pi/8$ . When these samples are flipped vertically or horizontally to let incident lights propagate from the inverse sides, the optical axis from A to H varies from  $0$  to  $\pi/2$ , and the polarization angles after samples A-H will vary from  $0$  to  $-\pi$ , having the inverse tendency compared with the samples without flipping. This property is the same as in classical half-wave plates.

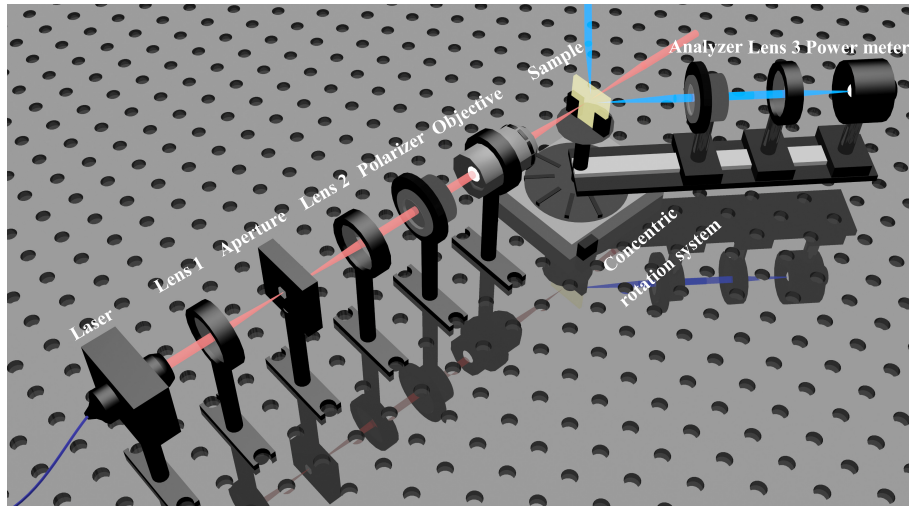


Figure S5: A schematic configuration of the experimental setup.